Enhanced Intersystem Crossing in Carbonylpyrenes

*Shinaj K. Rajagopal, Ajith R. Mallia and Mahesh Hariharan**

School of Chemistry, Indian Institute of Science Education and Research Thiruvananthapuram, Maruthamala P.O., Vithura, Thiruvananthapuram 695551, Kerala, India

Electronic Supplementary Information

Materials and methods:

Pyrene (98%), acetyl chloride (98%) and aluminum chloride (99.99%) were purchased from Sigma Aldrich and used as such without further purification. Carbon disulfide used as a solvent for the reaction was dried and distilled by standard procedure. TLC analysis were performed on precoated aluminum plates of silica gel 60 F254 plates (0.25 mm, Merck) and developed TLC plates were visualized under short and long wavelength UV lamps. Flash column chromatography was performed using silica gel of 200-400 mesh employing a solvent polarity correlated with the TLC mobility observed for the substance of interest. Yields refer to chromatographically and spectroscopically homogenous substances. Melting points (mp) were obtained using a capillary melting point apparatus and are reported without correction. IR spectra were recorded on a Shimadzu IRPrestige-21 FT-IR spectrometer as neat KBr pellets for all the derivatives. ^{1}H and ^{13}C NMR spectra were measured on a 500 MHz and 125 MHz Bruker avance DPX spectrometer respectively and 1,1,1,1-tetramethylsilane (TMS) is used as the internal standard for ^{1}H and ^{13}C NMR measurements. CHN analyses were carried out on an Elementar vario MICRO cube Elemental Analyzer. All values recorded in elemental analyses are given in percentages. High Resolution Mass Spectra (HRMS) were recorded on Agilent 6538 Ultra High Definition (UHD) Accurate-Mass Q-TOF-LC/MS system using either atmospheric pressure chemical ionization (APCI) or electrospray ionization (ESI) mode.

Spectral Measurements:

Absorption spectra were recorded on Shimadzu UV-3600 UV-VIS-NIR while fluorescence and excitation spectra were performed on Horiba Jobin Yvon Fluorolog spectrometers respectively. The excitation wavelength used is 350 nm unless otherwise mentioned. Fluorescence lifetime measurements were carried out in an IBH picosecond single photon counting system. The fluorescence decay profiles were de-convoluted using IBH data station software version 2.1, and fitted with exponential decay, minimizing the $\chi 2$ values of the fit to 1 ± 0.05. All spectroscopic experiments were performed by using standard quartz cuvettes of path length 1cm for solution in dried and distilled solvents. The excitation laser used is 375 nm with a pulse width of less than 100 ps. 1-4AP derivatives in chloroform were found to have lifetime significantly shorter than the excitation pulse width. The solution state fluorescence quantum yields were determined by using optically matched solutions. Quinine sulfate dissolved in 0.5 M H_2SO_4 (Φ_f = 0.546)[1] is used as the standard for 1-4AP derivatives.

Cyclic Voltammetry (CV): Electrochemical measurements were performed on a BASi (Bioanalytical Systems, Inc.) C-3 cell stand controlled by Epsilon electrochemical workstation. A three electrode

system is then constructed constituting a glassy carbon as the working electrode, a platinum-wire as the counter electrode, and an Ag/Ag+ (3 M NaCl) as the reference electrode. The electrochemical measurements were conducted under nitrogen atmosphere (5 psi, 10 minutes) in a deoxygenated anhydrous acetonitrile of tetra-n-butylammonium hexafluorophosphate (supporting electrolyte, 0.1 M) for monomer, and in $CHCl_3$ for aggregate with a scan rate of 50–100 mV s^{-1}. Calibration of the instrument was performed using the ferrocene/ferrocenium (Fc/Fc^+) redox couple as an internal standard and measured under same condition before and after the measurement of samples. The energy level of Fc/Fc^+ was assumed to be –4.8 eV with respect to vacuum. The half-wave potential of Fc/Fc^+ was estimated to be 0.5 V with reference to the Ag/Ag^+ electrode.
The HOMO and LUMO energy levels were calculated from the following equations:

$$E_{HOMO} = -(E_{ox}^{onset} + 4.8)\ \text{eV} \quad \text{and} \tag{1}$$

$$E_{LUMO} = -\left(E_{red}^{onset} + 4.8\right)\ \text{eV} \tag{2}$$

respectively, where E_{ox}^{onset} and E_{red}^{onset} are the onset oxidation and reduction potentials relative to the Ag/Ag^+ reference electrode.
The electrochemical energy gap (E_g) is estimated as follows:

$$E_g = (E_{LUMO} - E_{HOMO})\ \text{eV} \tag{3}$$

where E_{LUMO} and E_{HOMO} are the corresponding to HOMO and LUMO energy levels calculated after converting the values in Ag/Ag^+ with respect to the standard calomel electrode (SCE) convention.

Determination of fluorescence quantum yield and radiative and non-radiative rate constants: Solution state fluorescence quantum yields of 1-4AP derivatives were calculated by relative quantum yield method as follows,

$$\Phi_s = \Phi_{ref}\left(\frac{I_s}{I_{ref}}\right)\left(\frac{OD_{ref}}{OD_s}\right)\left(\frac{n_s}{n_{ref}}\right)^2 \tag{4}$$

wherein, Φ_s and Φ_{ref} are the quantum yields of sample and reference respectively, I_s and I_{ref} are the area under the emission spectrum for sample and reference respectively. OD_s and OD_{ref} are the absorbances of sample and reference respectively at the excitation wavelength. n_s and n_{ref} are the refractive index of the solvent in which sample and reference are taken.
Radiative (k_r) and non-radiative (k_{nr}) rate constants from the singlet excited states are calculated from the fluorescence quantum yields, Φ_f

$$\Phi_f = \frac{k_r}{k_r + k_{nr}} \tag{5}$$

The rate constants k_r and k_{nr} can be evaluated by measuring fluorescence lifetimes (τ_f) from TCSPC measurements. The following equations depict relation between Φ_f, τ_f, k_r and k_{nr}.

$$k_r = \frac{\Phi_f}{\tau_f} \quad \text{and} \tag{6}$$

$$k_{nr} = \frac{1 - \Phi_f}{\tau_f} \tag{7}$$

a change in Φ_f could be attributed to the changes in either k_r/k_{nr}. The enhancement in the quantum yield (Φ_f) with increased solvent polarity is due to the stabilization of the excited states by virtue of interaction with the solvent dipoles and decrease in the non-radiative (k_{nr}) rate constant.

Table S1. Electrochemical experimental and calculated energy levels of carbonylpyrens (1–4AP).

			Energy levels (eV)			Energy levels (eV)		
	E_{on}^{ox} (eV) [a]	E_{on}^{red} (eV) [a]	E_{HOMO} (eV) [a]	E_{LUMO} (eV) [a]	ΔE (eV)[a]	E_{HOMO} (eV)[b]	E_{LUMO} (eV)[b]	ΔE (eV)[b]
1AP	1.483	-1.562	-6.283	-3.238	3.045	-5.834	-2.278	3.555
2AP	1.579	-1.306	-6.379	-3.494	2.885	-6.044	-2.611	3.432
2'AP	1.578	-1.290	-6.378	-3.51	2.868	-6.064	-2.676	3.387
2''AP	1.612	-1.344	-6.412	-3.456	2.956	-6.076	-2.704	3.372
3AP	1.724	-1.107	-6.524	-3.693	2.831	-6.260	-2.977	3.283
4AP	1.8	-1.0	-6.60	-3.80	2.80	-6.436	-3.241	3.194
[a] experimental data; [b]computational data								

Table S2. Photophysical properties of carbonylpyrens (1–4AP) in $CHCl_3$.

	$^a\lambda_{abs}$ (nm)	$^a\lambda_f$ (nm)	$^a\Phi_f$	$^a\tau_f$(ns) [Amplitude] (%)	$^a\lambda_T$ (nm)	$^a\Phi_T$
P	337	393	0.60[2]	150.1 [100]	415	38.0[3]
1AP	359	412	0.004	1.39 [93] 0.98 [7]	450	52.30
2AP	373	426	0.008	1.39 [93] 0.65 [7]	450	90.09
2'AP	369	420	0.002	1.3 [80] 1.62 [20]	450 480 540	96.06
2"AP	375	413	0.008	1.4 [97] 0.6 [3]	490	94.53
3AP	388	431	0.003	0.9	460 490	96.45
4AP	407	435	0.002	0.6	470 500	97.03
[a]chloroform solution; abs – absorption; f – fluorescence; Φ- quantum yield; T- triplet						

Table S3. Excitation energy, oscillator strength, main transition orbital, and their contribution calculated for carbonylpyrenes (1–4AP) using TD-DFT (B3LYP/6-311+G(d,p)).

AP derivatives	State	Excitation Energy (eV)	Oscillator strength (*f*)	Main transition orbital	Characteristic orbitals involved	Contribution
P	T4	3.5953		HOMO-1→LUMO	π-π*	0.57309
	T3	3.5686		HOMO→LUMO+2	π-π*	0.51608
	T2	3.4472		HOMO→LUMO+1	π-π*	0.57142
	T1	2.1566		HOMO→LUMO	π-π*	0.68533
	S4	4.6312	0.0000	HOMO-2→LUMO	π−π*	0.68233
	S3	4.3758	0.0000	HOMO→LUMO+2	π−π*	0.68393
	S2	3.7618	0.0003	HOMO→LUMO+1	π−π*	0.52179
	S1	3.6976	0.2523	HOMO→LUMO	π−π*	0.66986
1AP	T4	3.4882		HOMO→LUMO+1	π−π*	0.50967
	T3	3.3018		HOMO-2→LUMO	n−π*	0.47969
	T2	3.0798		HOMO-1→LUMO	π−π*	0.50416
	T1	2.0137		HOMO→LUMO	π−π*	0.68261
	S4	4.2526	0.0189	HOMO-3→LUMO	π−π*	0.53272
	S3	3.6842	0.0250	HOMO-1→LUMO	π−π*	0.31142
				HOMO-2→LUMO	n−π*	-0.47754
	S2	3.5368	0.0042	HOMO-1→LUMO	π−π*	0.48744
				HOMO-2→LUMO	n−π*	-0.41107
	S1	3.3811	0.3305	HOMO→LUMO	π−π*	0.66907
				HOMO-2→LUMO	n−π*	-0.10680
2AP	T4	3.2322		HOMO-2→LUMO	π−π*	0.61257
	T3	3.1466		HOMO-3→LUMO	n−π*	0.55422
	T2	2.9366		HOMO-1→LUMO	π−π*	0.62909
	T1	1.9407		HOMO→LUMO	π−π*	0.68630
	S4	3.5789	0.0014	HOMO-2→LUMO	π−π*	0.55139
	S3	3.5775	0.0175	HOMO-3→LUMO	π−π*	0.63612
				HOMO-3→LUMO+1	n−π*	0.14633
				HOMO-3→LUMO+3	n−π*	0.13415

	S2	3.3534	0.0103	HOMO-1→LUMO	π−π*	0.60578
				HOMO-3→LUMO+1	n−π*	0.10768
	S1	3.2621	0.3659	HOMO→LUMO	π−π*	0.67578
				HOMO-3→LUMO	n−π*	0.10625
2'AP	T4	3.2122		HOMO-3→LUMO	π−π*	0.58217
	T3	3.0649		HOMO-2→LUMO	n−π*	0.56224
	T2	2.9569		HOMO-1→LUMO	π−π*	0.63426
	T1	1.9112		HOMO→LUMO	π−π*	0.68667
	S4	3.6180	0.0440	HOMO-3→LUMO	π−π*	0.55533
				HOMO-2→LUMO+1	n−π*	-0.16268
	S3	3.5039	0.0000	HOMO-1→LUMO+1	π−π*	0.12522
				HOMO-2→LUMO	n−π*	0.64427
				HOMO-2→LUMO+4	n−π*	0.11443
	S2	3.3982	0.0121	HOMO-1→LUMO	π−π*	0.58073
				HOMO-2→LUMO+1	n−π*	0.15708
	S1	3.2178	0.4263	HOMO→LUMO	π−π*	0.67433
2"AP	T4	3.1900		HOMO-3→LUMO	π−π*	0.57896
	T3	3.0655		HOMO-2→LUMO	n−π*	0.58915
	T2	2.9120		HOMO-1→LUMO	π−π*	0.61645
	T1	1.9024		HOMO→LUMO	π−π*	0.68751
	S4	3.5600	0.0023	HOMO-3→LUMO	π−π*	0.54376
				HOMO-2→LUMO+1	n−π*	0.13380
	S3	3.4762	0.0186	HOMO-3→LUMO+1	π−π*	0.18320
				HOMO-2→LUMO	n−π*	0.64141
				HOMO-2→LUMO+4	n−π*	0.10058
	S2	3.3842	0.0122	HOMO-1→LUMO	π−π*	0.56911
				HOMO-2→LUMO+1	n−π*	0.14953
	S1	3.2101	0.4039	HOMO→LUMO	π−π*	0.67743
				HOMO-2→LUMO	n−π*	-0.11239
3AP	T4	3.0768		HOMO-3→LUMO	n−π*	0.53675
	T3	2.9932		HOMO-2→LUMO	π−π*	0.53079
	T2	2.8060		HOMO-1→LUMO	π−π*	0.65503
	T1	1.8452		HOMO→LUMO	π−π*	0.68923
	S4	3.4711	0.0127	HOMO-2→LUMO+1	π−π*	0.10497

				HOMO-3→LUMO	n–π*	0.58851
				HOMO-3→LUMO+2	n–π*	0.11392
	S3	3.3850	0.0091	HOMO-2→LUMO	π–π*	0.58001
	S2	3.2210	0.0174	HOMO-1→LUMO	π–π*	0.62544
	S1	3.1141	0.4384	HOMO→LUMO	π–π*	0.67619
				HOMO-3→LUMO	n–π*	-0.10453
4AP	T4	3.0880		HOMO-3→LUMO	n–π*	0.64605
	T3	2.8940		HOMO-2→LUMO	n–π*	0.60853
	T2	2.6939		HOMO-1→LUMO	π–π*	0.66586
	T1	1.7869		HOMO→LUMO	π–π*	0.69059
	S4	3.3928		HOMO-5→LUMO	n–π*	0.65801
				HOMO-3→LUMO+2	n–π*	0.15263
	S3	3.2238	0.0000	HOMO-1→LUMO+2	π–π*	-0.11103
				HOMO-2→LUMO	n–π*	0.67264
	S2	3.0911	0.0234	HOMO-1→LUMO	π–π*	0.65083
				HOMO-2→LUMO+2	n–π*	-0.10473
				HOMO-4→LUMO	n–π*	-0.17373
	S1	3.0184	0.4624	HOMO→LUMO	π–π*	0.67757
				HOMO-3→LUMO	n–π*	0.13654

Table S4. Lifetimes obtained from global analyses of nanosecond laser flash photolysis of carbonylpyrenes (1–4AP) in $CHCl_3$ (λ_{exc}=355 nm).

	Time (μs) V_1 (After N_2 purging)	Time (ns) V_2 (After O_2 purging)
1 AP	4.85	42.1
2 AP	5.76	60.9
2’ AP	7.04	32.6
2” AP	10.13	50.2
3 AP	11.08	40.2
4 AP	12.16	46.0

Table S5. Lifetimes of carbonylpyrenes (1–4AP) obtained from global analyses of fTA spectra (λ_{exc}=400 nm).

	V_1 (ps)		V_2 (ns)
	τ_1 ($S_p \leftarrow S_q$)*	τ_2	$\tau_3{}^{\perp}$
AP	0.54 (76%)	9.08 (24%)	0.12
2 AP	0.70 (65%)	7.45 (35%)	0.27
2' AP	0.92 (54%)	10.28 (46%)	0.42
2" AP	0.43 (80%)	5.42 (20%)	0.48
3 AP	0.58 (78%)	11.27 (22%)	0.54
4 AP	1.40 (61%)	7.9 (39%)	1.96
*$q>p$; $^{\perp}$fTA measurements are performed without purging N_2 gas through the solutions of 1-4AP			

Table S6. Decay lifetime of phosphorescence of carbonylpyrenes (1–4AP) in $CHCl_3$ recorded at 77 K (λ_{exc}= 380 nm).

	Phosphorescence lifetime ($CHCl_3$) (μs)
1AP	12.7
2AP	9.8
2'AP	9.5
2"AP	11.3
3AP	9.4
4AP	11.4

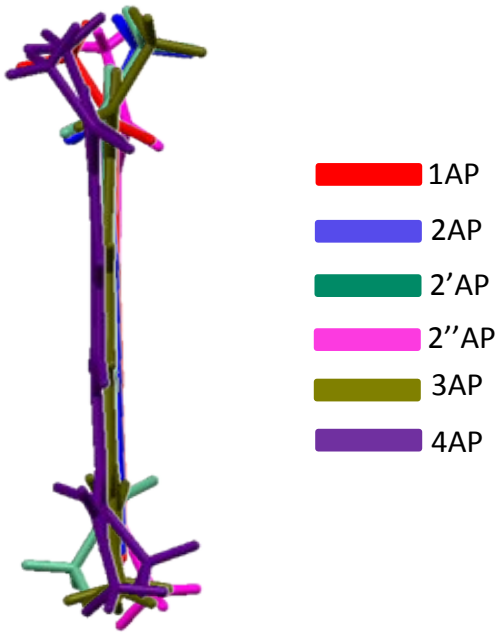

Fig. S1 Overlay of the side view of crystal structure of 1-4AP showing the torsion angle between the pyrene and carbonyl planes.

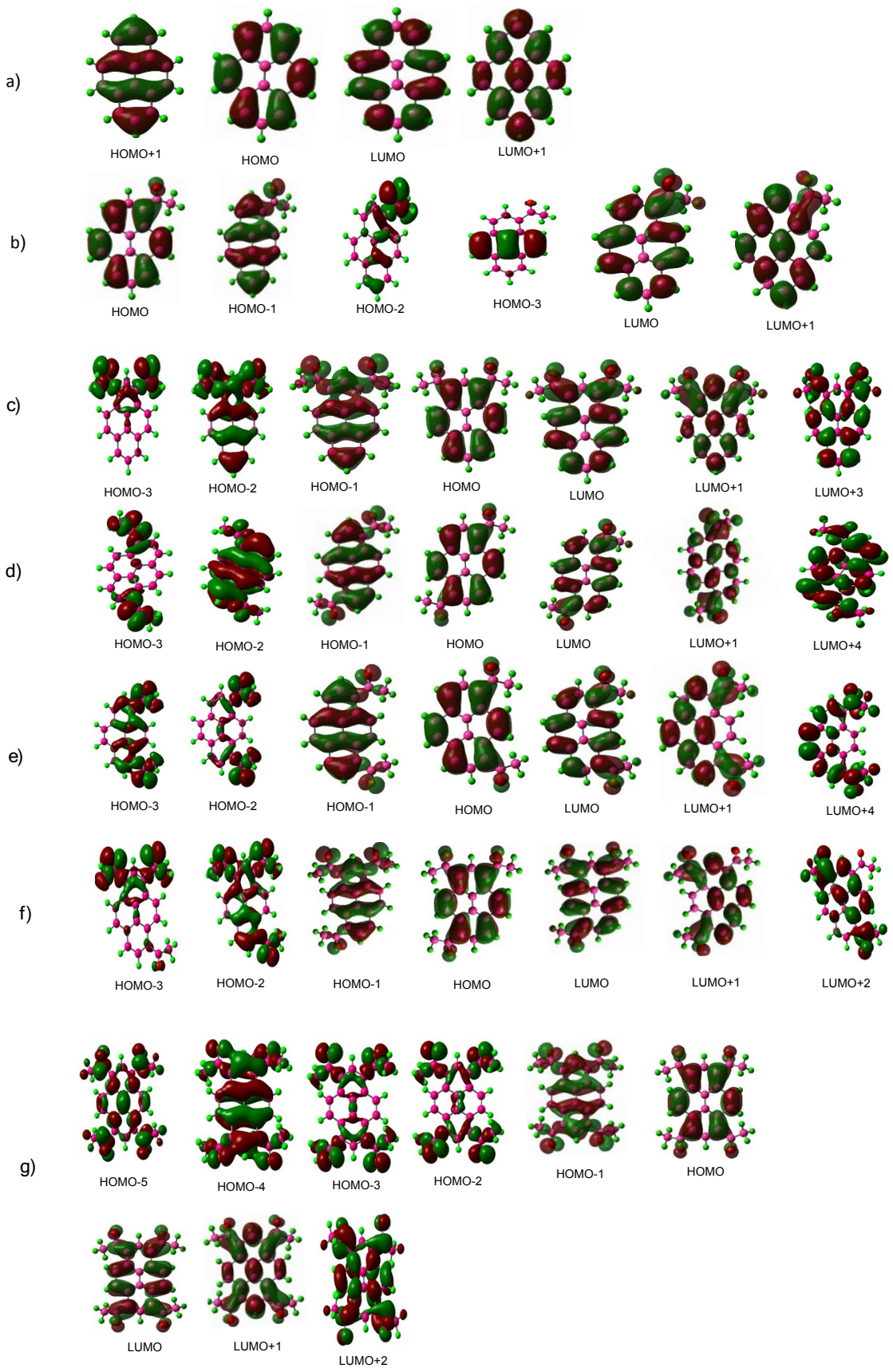

Fig. S2 Frontier molecular orbitals (FMO) of a) P, b) 1AP, c) 2AP, d) 2'AP, e) 2''AP, f) 3AP and g) 4AP involved in the excited state transitions.

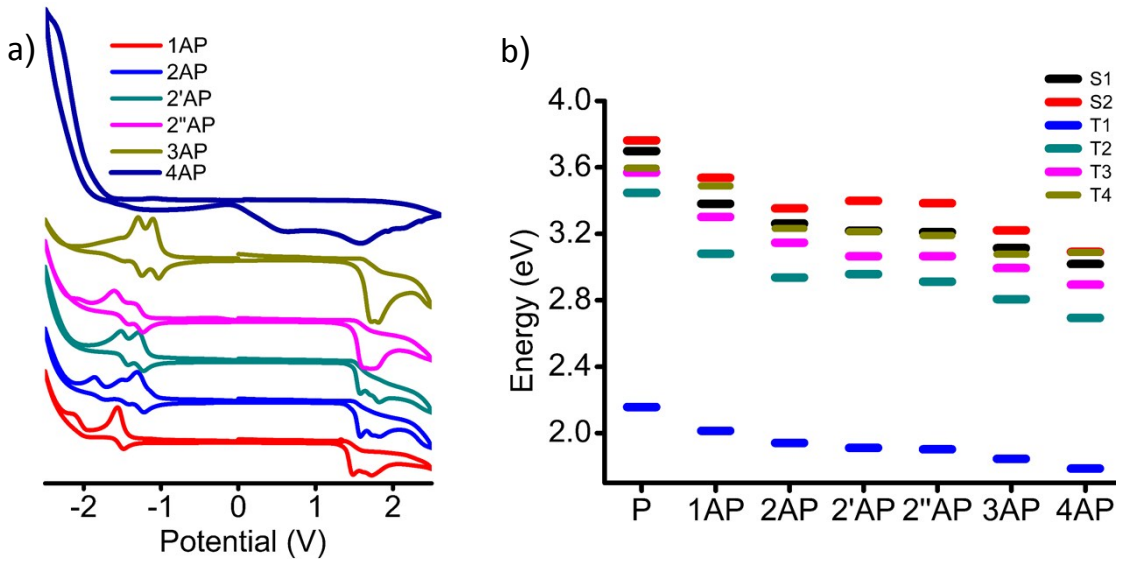

Fig. S3 Shows a) Cyclic voltammograms of 1–4AP derivatives in CH_3CN and b) Energy level diagram for 1-4AP derivatives as calculated using TD-DFT (B3LYP/6-311+G(d,p)).

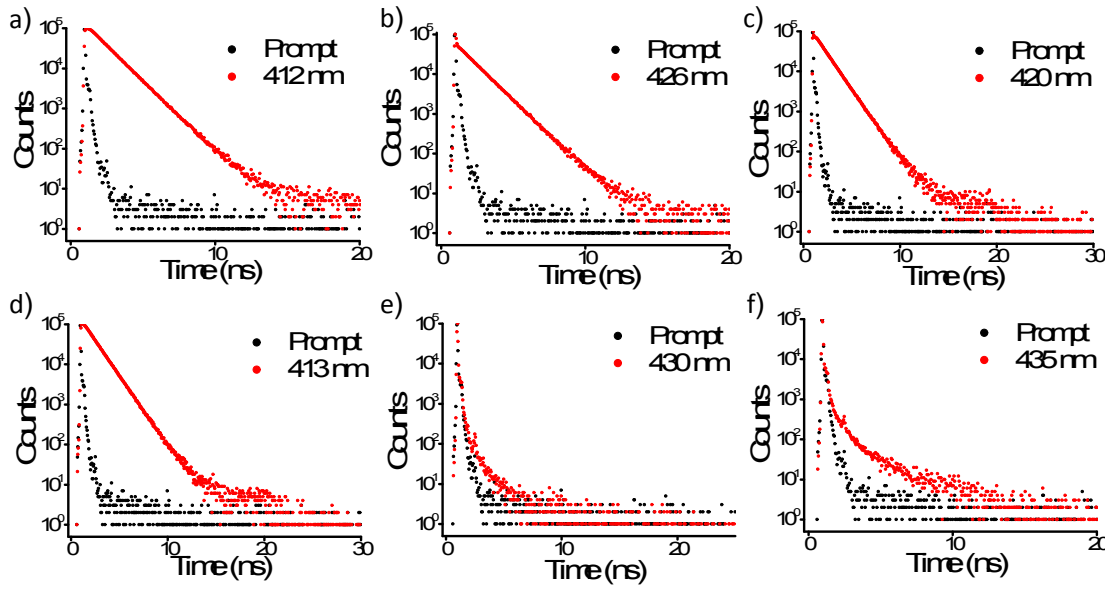

Fig. S4 Shows fluorescence decay profile of a) 1AP, b) 2AP, c) 2'AP, d) 2"AP, e) 3AP and f) 4AP in $CHCl_3$ solution on exciting at 375 nm and collected at respective emission maximum.

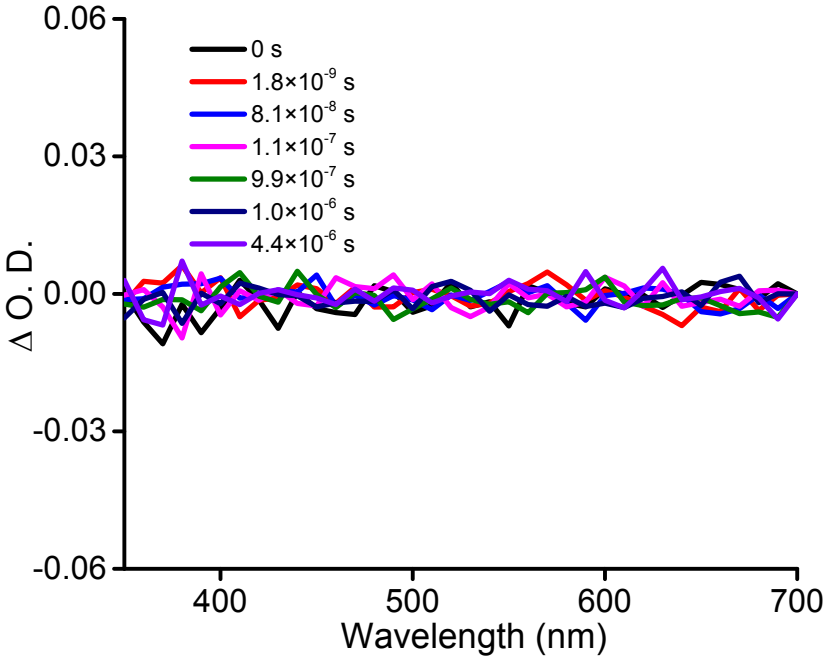

Fig. S5 Shows transient absorption was readily quenched by the dissolved oxygen in 4AP thus suggesting that the transient species may be due to the triplet excited state.

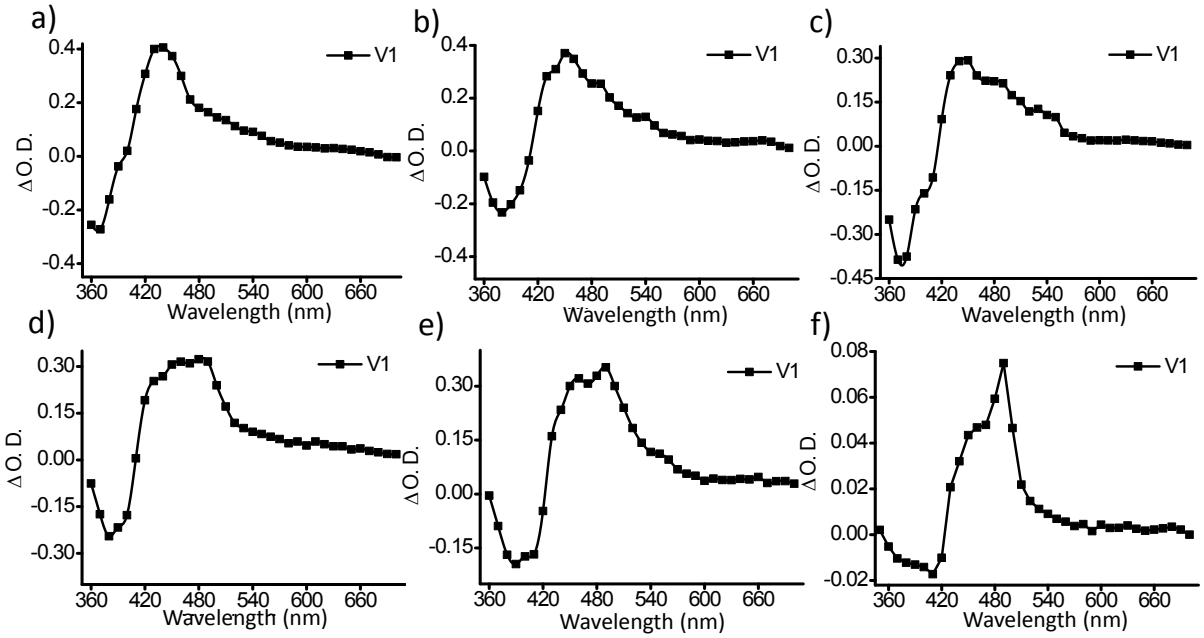

Fig. S6 Right singular vectors obtained from global analyses of nTA measurement for a) 1AP, b) 2AP, c) 2'AP, d) 2"AP, e) 3AP and f) 4AP derivatives in $CHCl_3$.

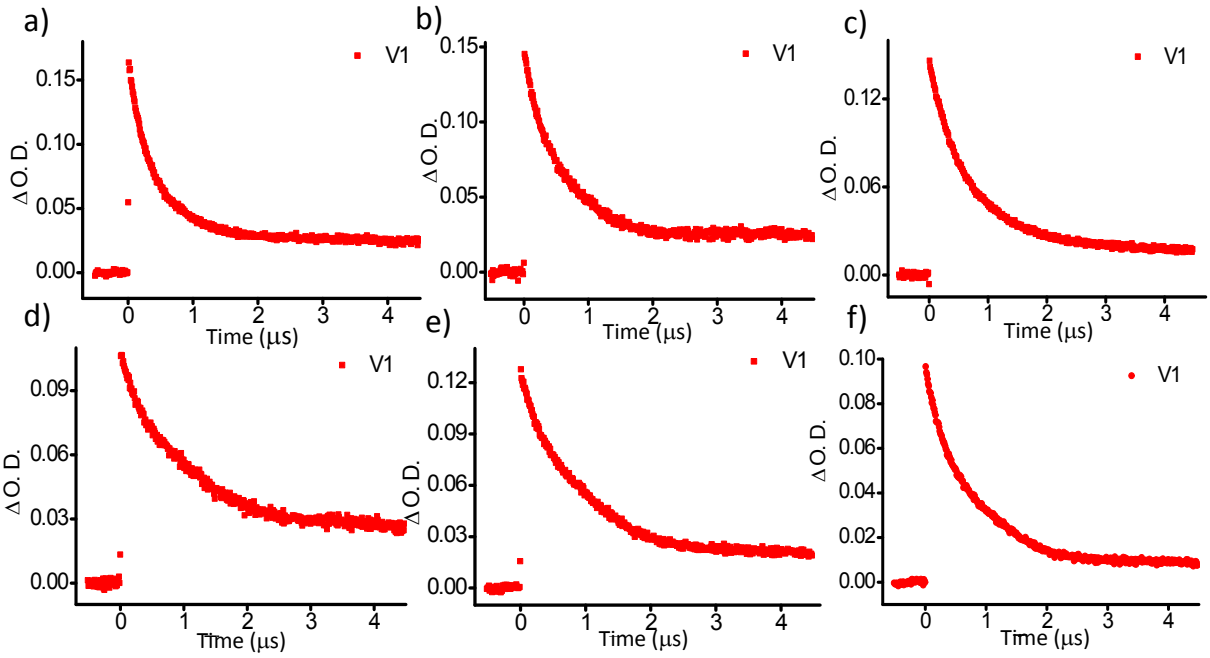

Fig. S7 Kinetic decay profiles corresponding to the right singular vectors obtained from global analyses for a) 1AP, b) 2AP, c) 2'AP, d) 2"AP, e) 3AP and f) 4AP derivatives in $CHCl_3$.

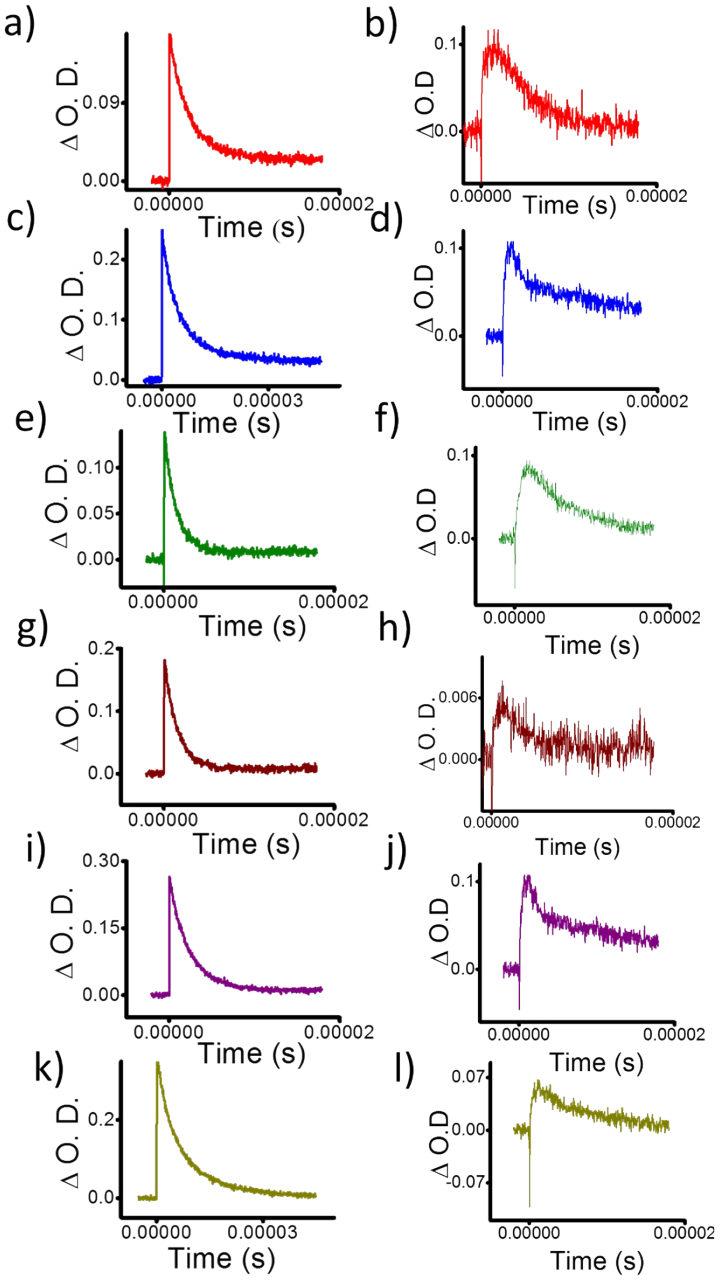

Fig. S8 Shows a) 1AP, c) 2AP, e) 2'AP, g) 2''AP, i) 3AP and k) 4AP decay of the transient decay at the respective triplet absorption and b) 1AP, d) 2AP, f) 2'AP, h) 2''AP, j) 3AP and l) 4AP shows the transient decay at 510 nm.

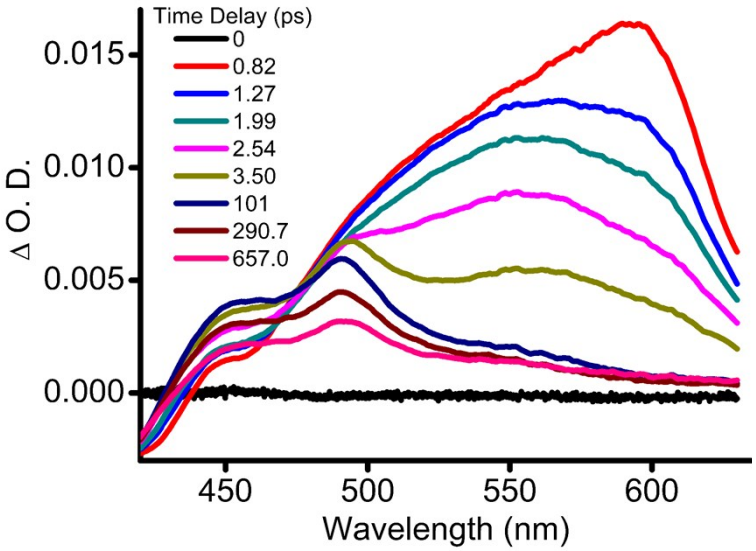

Fig. S9 Transient absorption spectra for 4AP as plotted in the early time delay where at 3.5 ps a growth around 500 nm is observed.

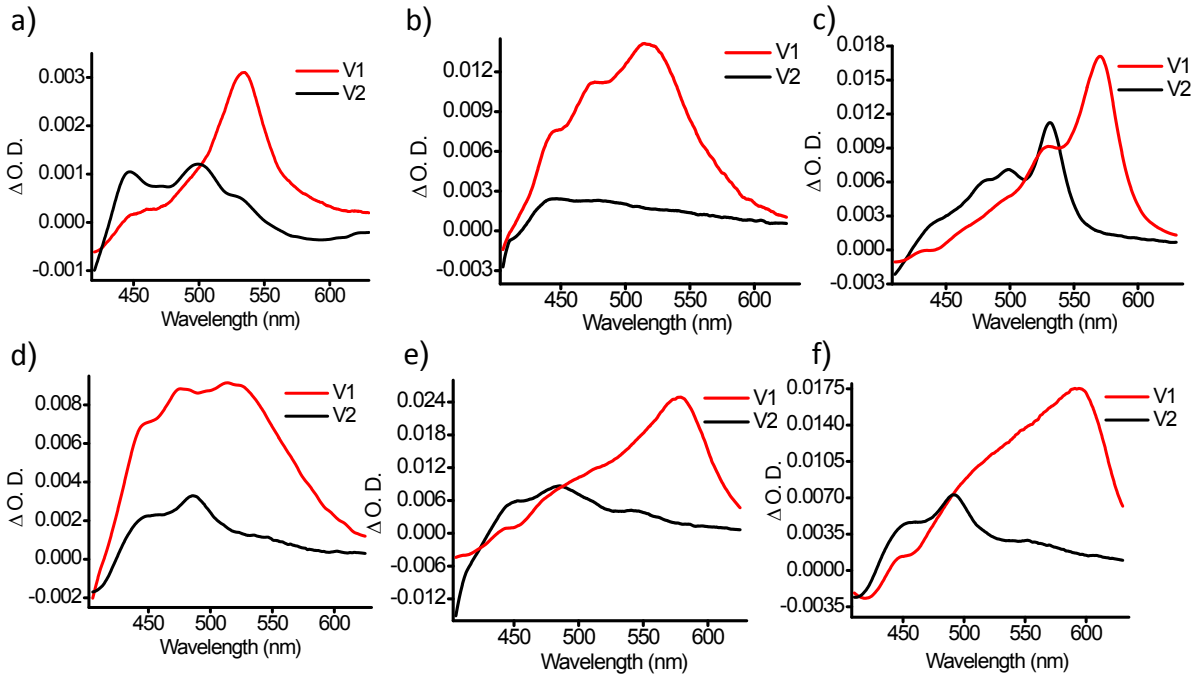

Fig. S10 Right singular vectors obtained from global analyses of fTA measurement for a) 1AP, b) 2AP, c) 2'AP, d) 2"AP, e) 3AP and f) 4AP derivatives in $CHCl_3$.

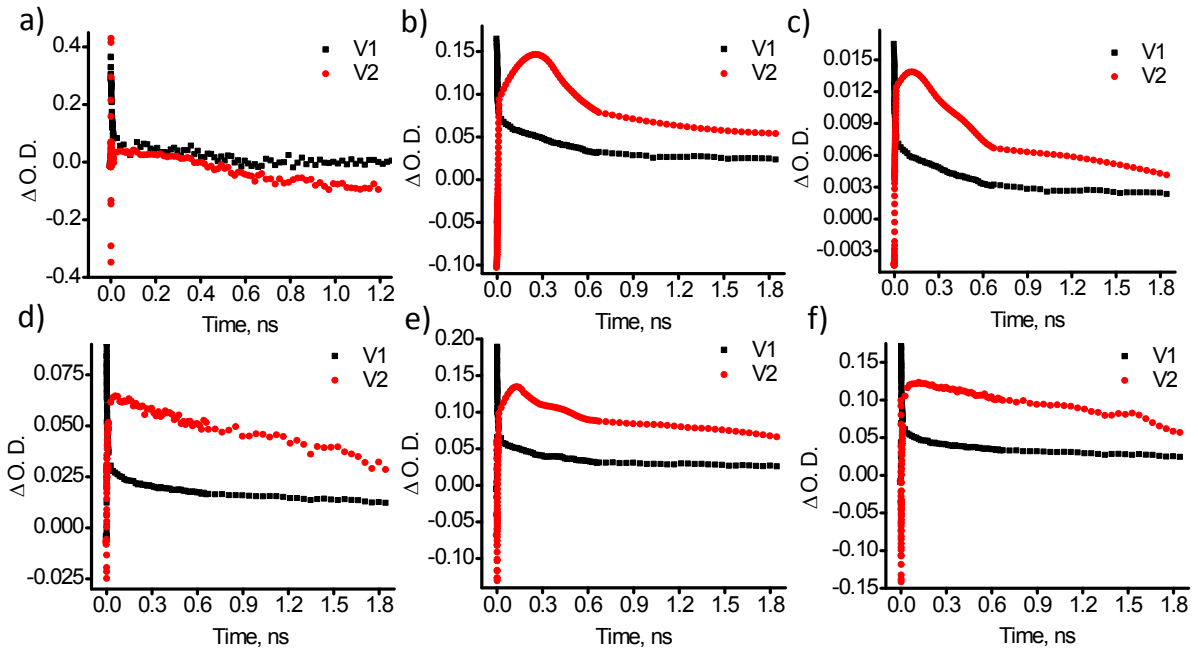

Fig. S11 Kinetic decay profiles corresponding to the right singular vectors obtained from global analyses for a) 1AP, b) 2AP, c) 2'AP, d) 2"AP, e) 3AP and f) 4AP derivatives in $CHCl_3$.

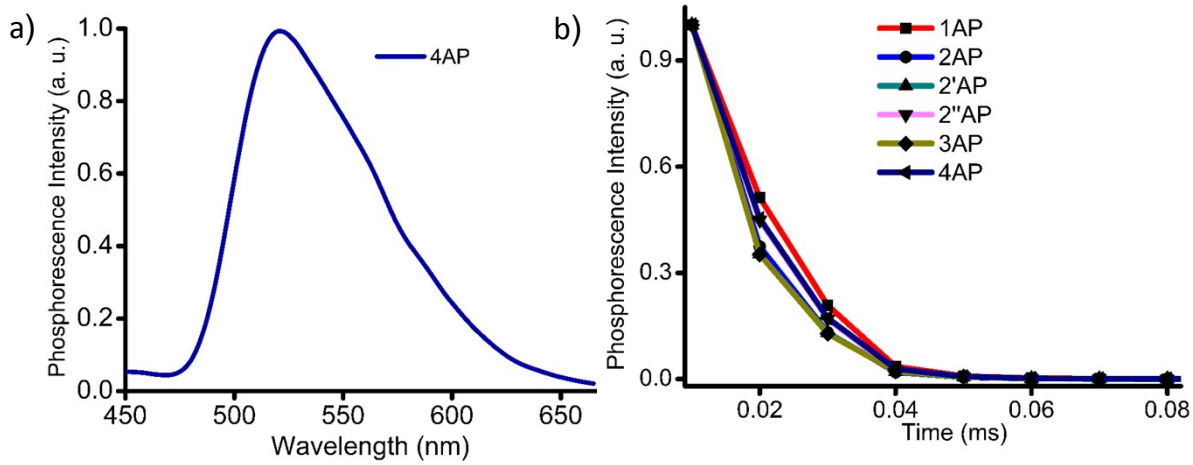

Fig. S12 a) Phosphorescence spectrum of 4AP in $CHCl_3$ recorded at 77 K (λ_{ex} = 380 nm) and b) Phosphorescence decay of carbonylpyrenes (1–4AP) in $CHCl_3$ recorded at 77 K (λ_{ex} = 380 nm).

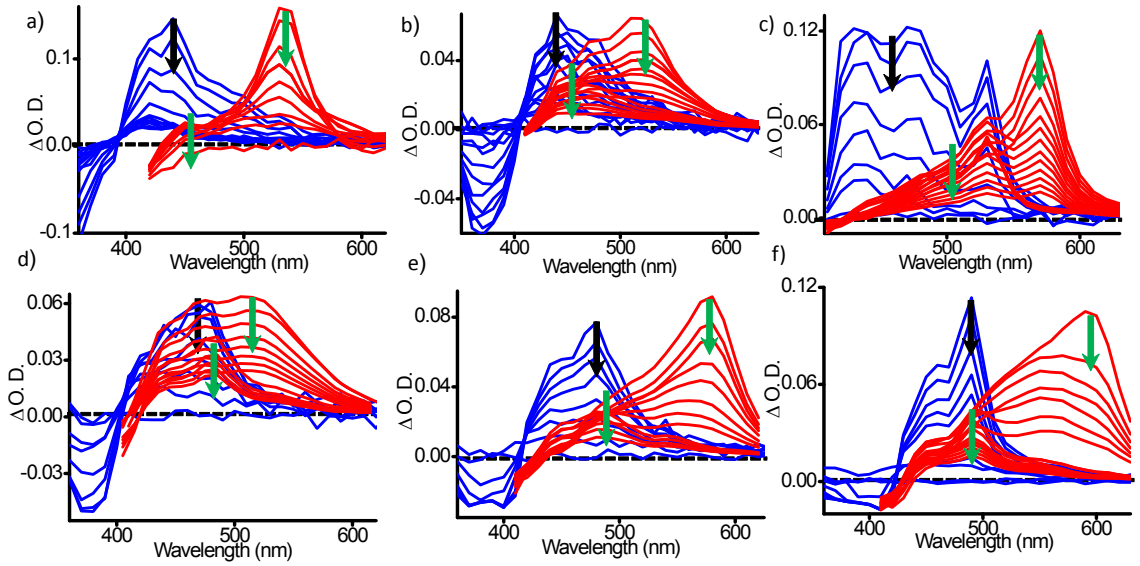

Fig. S13 Overlay of nanosecond (blue trace) and femtosecond (red trace) transient absorption spectra of a) 1AP, b) 2AP, c) 2'AP, d) 2''AP, e) 3AP and f) 4AP derivatives in $CHCl_3$. Black arrow indicate the decay in the nanosecond transient absorption while the green arrow indicates the decay of the femtosecond transient absorption bands.

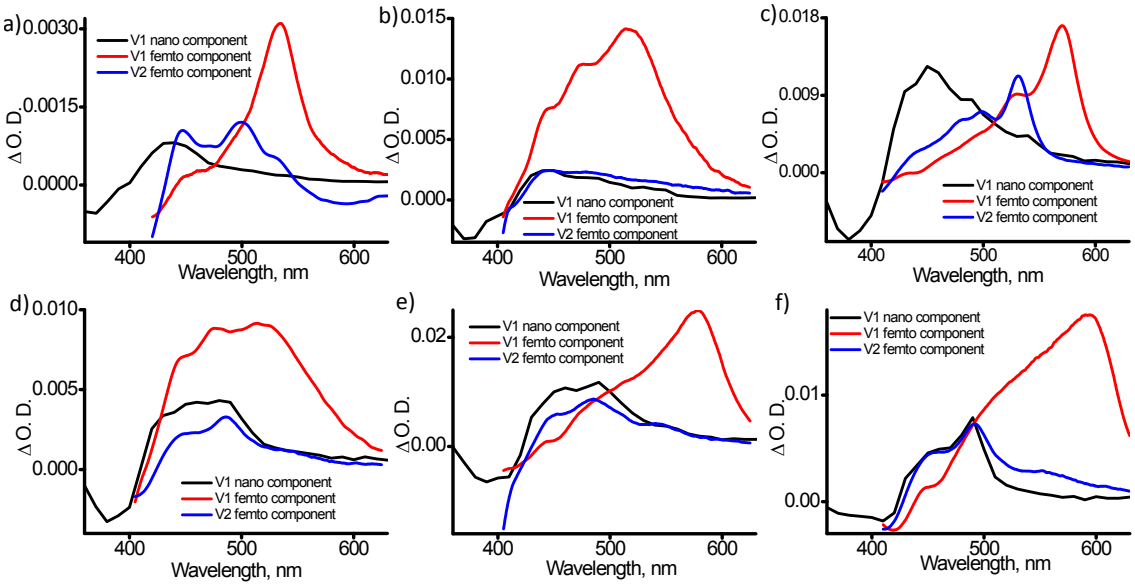

Fig. S14 Overlay of SVD of nanosecond and femtosecond transient spectra of a) 1AP, b) 2AP, c) 2'AP, d) 2"AP, e) 3AP and f) 4AP derivatives in $CHCl_3$.

References:

1. D. F. Eaton, *Pure Appl. Chem*, 1988, **60**, 1107-1114.
2. R. Katoh, S. Sinha, S. Murata and M. Tachiya, *J. Photochem. Photobiol. A: Chem.*, 2001, **145**, 23-34.
3. T. Medinger and F. Wilkinson, *Trans. Faraday Soc.*, 1966, **62**, 1785-1792.